A STUDY OF SECONDARY AIR INJECTION INTO A TWO-DIMENSIONAL CONVERGING-DIVERGING NOZZLE

By

ROGER O. WARLOE

Bachelor of Arts

University of California at Los Angeles

Los Angeles, California

1955

Submitted to the Faculty of the Graduate School of
the Oklahoma State University
in partial fulfillment of the requirements
for the degree of
MASTER OF SCIENCE
August, 1963

OKLAHOMA
STATE UNIVERSITY
LIBRARY

JAN 9 1964

A STUDY OF SECONDARY AIR INJECTION INTO A TWO-DIMENSIONAL CONVERGING-DIVERGING NOZZLE

Thesis Approved:

Glen W. Grummert
Thesis Adviser

D. R. Haworth

Dean of Graduate School

542226

ACKNOWLEDGMENT

The author wishes to express his gratitude to Dr. Glen W. Zumwalt, his adviser, for his invaluable guidance and assistance in preparation of this thesis. Acknowledgment is also extended to John M. Love, associate professor of Mechanical Engineering, University of Missouri, for guidance and help in conduction of the tests and measurements.

Gratitude is extended to the Mechanical Engineering Laboratory personnel and to the fine machinist, L. S. Benjamin, who manufactured the necessary parts used in this thesis project.

Appreciation is extended to the U. S. Air Force whose educational program made this advanced study possible.

In closing, appreciation is extended to Mrs. Claudine King for her excellent typing of the manuscript, and to my wife, Joan, for her hours of patience and understanding during the past two years.

TABLE OF CONTENTS

Chapter		Page
I.	INTRODUCTION	1
II.	ANALYSIS OF SECONDARY INJECTION	3
III.	TEST EQUIPMENT	7
IV.	TESTING PROCEDURE	17
V.	DISCUSSION OF RESULTS	20
VI.	CONCLUSIONS	30
	RECOMMENDATIONS	30
SELECTED BIBLIOGRAPHY		32
APPENDIX A		33

LIST OF TABLES

Table Page

I. Dimensionless Static Pressure Field with Injection at the Throat 28

LIST OF FIGURES

Figure Page

1. Approximate Flow Pattern with Secondary Injection in the Throat Region. 4

2. Schematic Diagram of Test Equipment 8

2a. Detail of Test Section. 9

3. Control Panel for Test Equipment. 10

4. Test Equipment Showing Right Side and Two-Position Valve. . . . 11

5. Test Equipment Showing Left Side and Settling Chamber 11

6. Throat Section, Nozzle Block and Left Side Wall 12

7. Exploded View of Switching Valve. 14

8. Reduction in Throat Area versus Secondary Mass Flow Rate for Upstream Injection 22

9. Reduction in Throat Area versus Secondary Mass Flow Rate for Downstream Injection 23

10. Reduction in Throat Area versus Injection Position. 24

11. Dimensionless Static Pressure Field with Injection at the Throat 27

LIST OF SYMBOLS

A	Throat area
A_1	Primary flow area
A_2	Secondary flow area
C_d	Flow coefficient
h	Throat height
$\dot{m}_o$	Theoretical mass flow rate with no secondary flow
$\dot{m}_1$	Primary mass flow rate
$\dot{m}_2$	Secondary mass flow rate
P	Static pressure
P_o	Stagnation pressure
R	Radius of curvature of nozzle walls
T_o	Stagnation temperature

Subscripts

1	primary
2	secondary

CHAPTER I

INTRODUCTION

Solid fuel rocket motors suffer from the lack of thrust magnitude control once the grain and nozzle have been assembled. This control is necessary in order to utilize the rocket motor during conditions of varying temperature and pressure. Additionally, the more powerful fuels, those with high specific impulse, are very pressure sensitive and cannot be used safely with a fixed area nozzle. These limitations could be overcome if the rocket motor utilized a variable throat area.

Mechanical controls of the throat area were proposed by: Berman and Crimp (1)[1], plug nozzle; Gates and Pinto (2), iris-type nozzle; and Rao (3), expansion-deflection. These proposals all share the problem of achieving satisfactory mechanical movement in the hot gas environment of the rocket motor.

Control of the throat area by secondary gas injection at the throat has been proposed by Zumwalt and Jackomis (4, 5). This control is called an aerodynamically-variable throat (AVT) nozzle (6). This system has the advantage of no moving parts in the high temperature environment. In addition, if a cold secondary gas were used, then the boundary layer at the throat would help prevent ablation and the change of the throat area as the rocket motor burned.

---

1 Refers to Selected Bibliography.

While the aerodynamic throat has been applied to many flow control devices for at least the past 25 years, the application to the solid propellant rocket motor seems to be one for which it is uniquely well suited (5). Similarly, the work presented herein may apply to any secondary injection in a transonic region, but it was specifically planned to aid in the development of thrust nozzle applications.

A two-dimensional study was chosen in order to understand better the flow field in a supersonic nozzle with secondary air injection. Half of a two-dimensional arc-shape nozzle was used since the flow pattern would be symmetrical across the centerline. The purpose was to determine the effectiveness of the secondary air injection in regulating the primary flow area for various injection positions and with varying secondary mass flow rates. In addition, the pressure field in the throat area was recorded with and without secondary injection in order to measure the changes induced by the higher pressure secondary fluid.

CHAPTER II

ANALYSIS OF SECONDARY INJECTION

Supersonic flow in a converging-diverging nozzle occurs with a strong pressure gradient. This favorable pressure drop accelerates the main flow as well as the boundary layer near the wall. For this reason, the boundary layer thickness at the throat of a rocket nozzle is normally negligible (Appendix A). However, with secondary fluid injection an effective step is formed which blocks the primary flow and causes an adverse pressure gradient. This in turn causes the boundary layer to grow, due to the lack of the highly favorable pressure gradient, and separation of the main flow away from the curved nozzle wall. A flow model of the AVT nozzle can be formulated on the basis of known flow characteristics in nozzle throats (7). This is shown in Figure 1. A local high pressure area probably exists in the separated region upstream of the point of injection. As the secondary mass flow is increased, this area of separation probably increases.

The velocity of the fluid at the throat is transonic with the flow accelerating to supersonic flow through a series of expansion waves. With secondary injection, the velocity field is no longer a smooth function of the static pressure as there are regions of primary flow, mixed flow, secondary flow, and separated (stagnated) flow. The thin boundary layer of the primary flow is lost in the mixing of the two fluids. The sonic line (local flow Mach number equal to one) bows slightly downstream

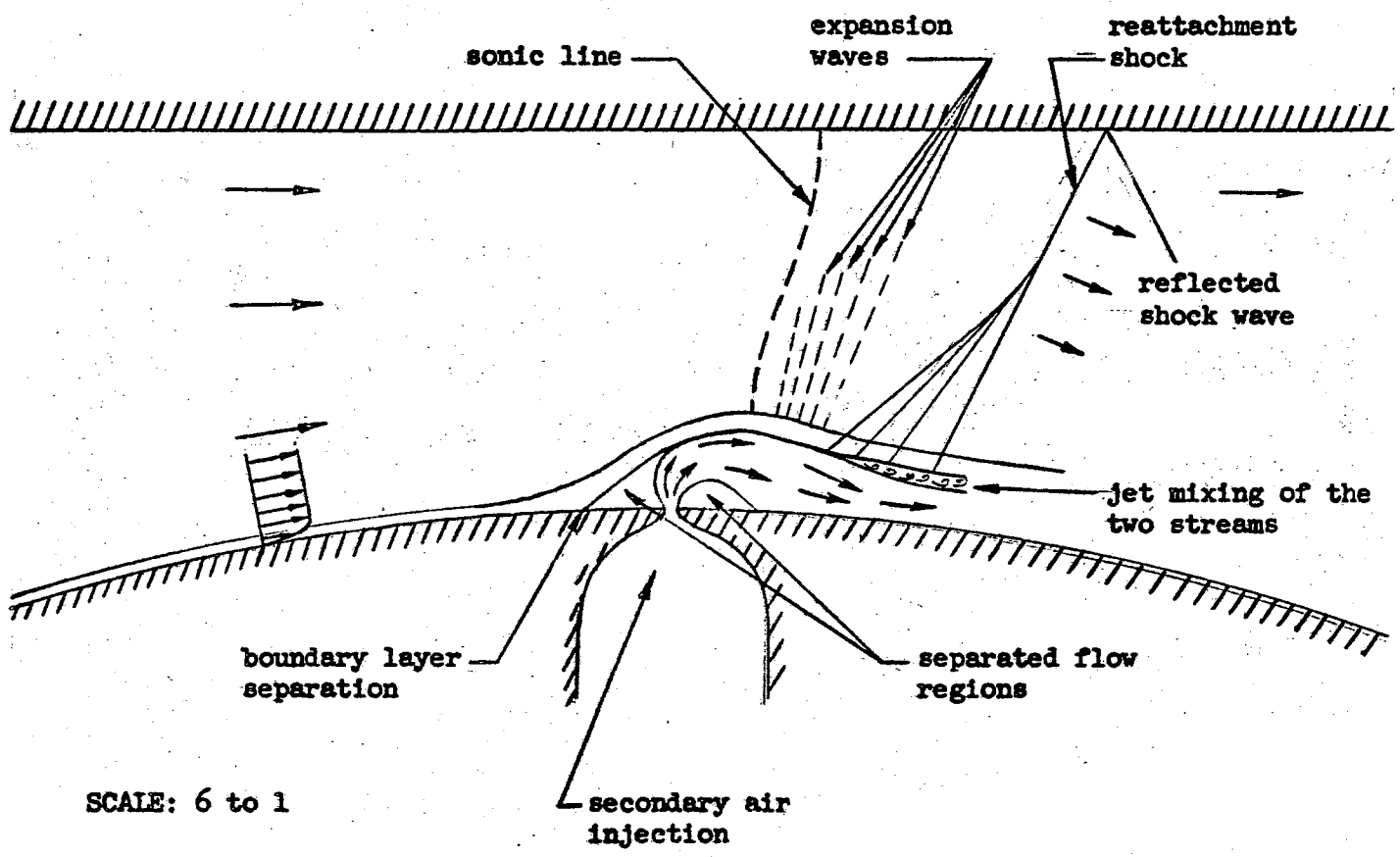

Figure 1. Approximate Flow Pattern with Secondary Injection in the Throat Region.

at the center from a straight line across the minimum area of the nozzle due to the curvature change of the streamlines from the axis to the wall.

Disturbances created by jet-mixing and the reattachment of the separated secondary flow behind the injection slit must be transmitted along Mach lines through the primary flow. If these are light shocks, they tend to coalesce in the non-uniform flow field.

Exact analytical analysis of the flow field along a curved wall with a strong pressure gradient is extremely complex; and with the addition of secondary injection into the main stream, analysis is almost impossible as there are likely to be regions of separation fore and aft of the point of injection. These effects have been observed in the hydraulic analogy to occur within a few slit widths from the injection (7). Additionally, the impingement of the secondary fluid on the primary flow with subsequent partial mixing varies as the position of injection and the amount of secondary mass change (6).

Following the approach of previous investigators, the measure of blockage effectiveness of the secondary stream is called the "magnification ratio." This is defined as the change in the mass flow rate of the primary fluid per unit flow rate of secondary fluid. This can also be expressed as the change in primary flow area.

The mixing of the two fluids makes it difficult to determine the loss of momentum of the primary flow to the secondary fluid. Momentum of the injected fluid was found by Jackomis (6) and Rodriguez (8) not to be a significant factor on the blockage effectiveness. Their tests were limited to small injection angles with the fluid injected at the throat of axisymmetric nozzles.

Tests conducted by Jackomis showed that the only significant parameter

for blockage effectiveness for a given injection location and angle was the ratio of secondary mass flow to primary mass flow ($\dot{m}_2/\dot{m}_o$). These tests used a variable slit width on an axisymmetric nozzle, with the secondary stagnation pressure controlled so that the range of secondary stagnation pressure to primary stagnation pressure ratio (P_{o2}/P_{o1}) was from one-half to two. For this pressure ratio range, the cross-stream momentum appeared not to be a significant variable. The same gas, cold air, was used in the primary and secondary streams. If gases of different physical and thermodynamic properties or high pressure secondary injection liquids were used, then there might be some correlation between magnification ratio and axial momentum of the secondary fluid.

Work by Rodriguez (8) on side injection at the throat resulted in no side force even when injection was not uniformly distributed around the axisymmetric nozzle. The added force (pressure times area) upstream, in the separated region, is offset by the reduced force downstream. His wall pressure data on axisymmetric nozzles showed however, that the increased pressure upstream and the decreased pressure downstream caused a thrust loss for the rocket nozzle when secondary injection was introduced.

Determination of the location of maximum "bulge" and the shape formed by the injected fluid is necessary to design the nozzle. If the bulge can be made to coincide with the minimum geometric cross section, then maximum blockage will result. Correlation between slit width, mass flow ratios, or wall curvature and the maximum bulge are areas to be explored. Another consideration is the effect on the primary stream pressure field when secondary injection occurs. At present, no literature can be found on these subjects.

CHAPTER III

TEST EQUIPMENT

The supersonic wind tunnel in the Mechanical Engineering Laboratory at Oklahoma State University was modified to run the test of cold secondary air injection into a two-dimensional converging-diverging nozzle. The arc radius to throat height ratio was 5.6 to 1. A schematic diagram of the test equipment is shown in Figure 2, with the detail drawing of the half-nozzle test section in Figure 2a. Pictures of the control panel, the left and right sides of the wind tunnel, and the open view of the test section are shown in Figures 3 through 6.

To modify the wind tunnel, the wind tunnel nozzle blocks and diffuser sections were removed, leaving an open channel approximately four and one-half inches high and one inch wide. A new inlet was formed by inserting flat blocks with rounded upstream sections. The resulting channel was then 1.9 inches high and 1 inch wide.

The half-nozzle was placed with its throat 6 inches downstream from the channel inlet. It was formed by a brass cylinder with a 1.875 inch radius on the bottom and a straight wall, acting as a centerline boundary, on top. The side walls were 1/2 inch aluminum plate. No correction for a boundary layer was made since calculations based on flow coefficients and theoretical boundary layer growth showed it to be negligible in the throat area (Appendix A). The throat height was 0.337 inches and the width 1.015 inches.

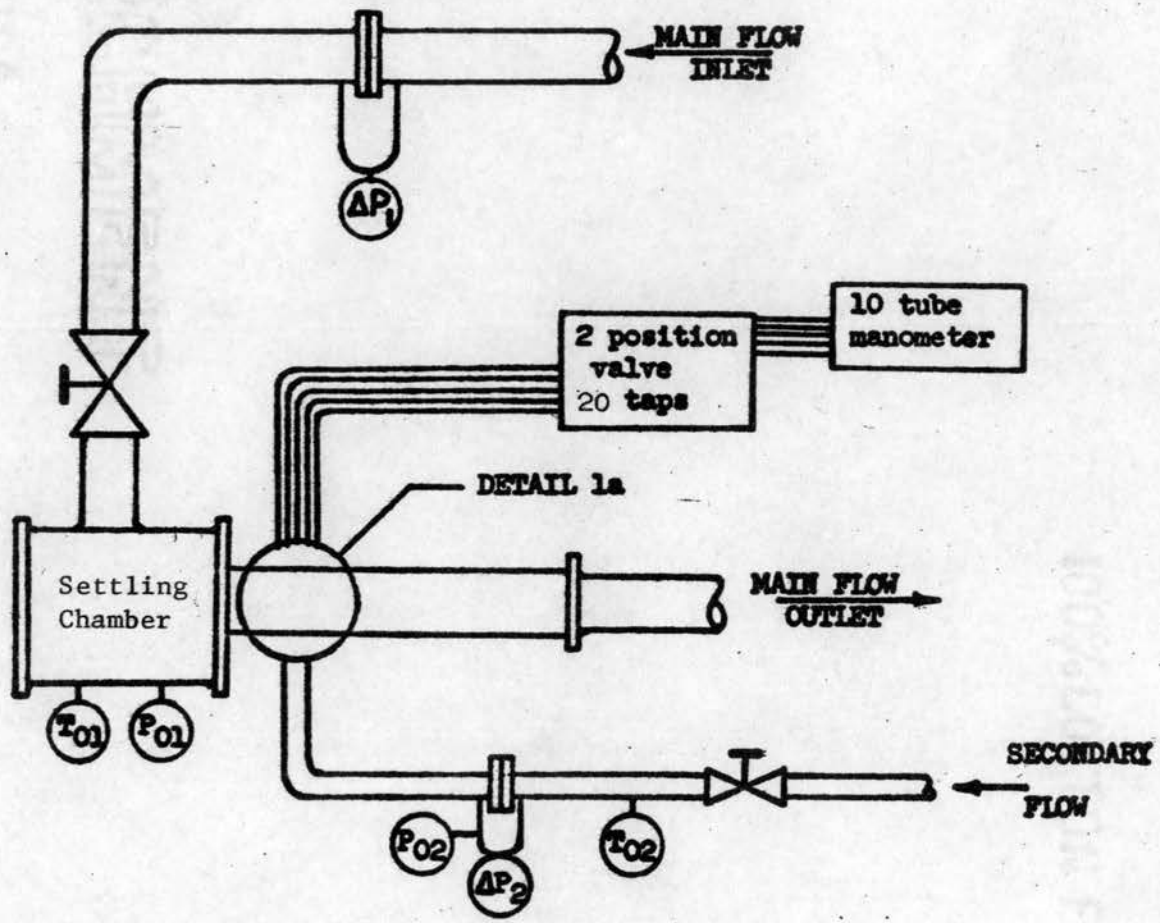

Figure 2. Schematic of Test Equipment.

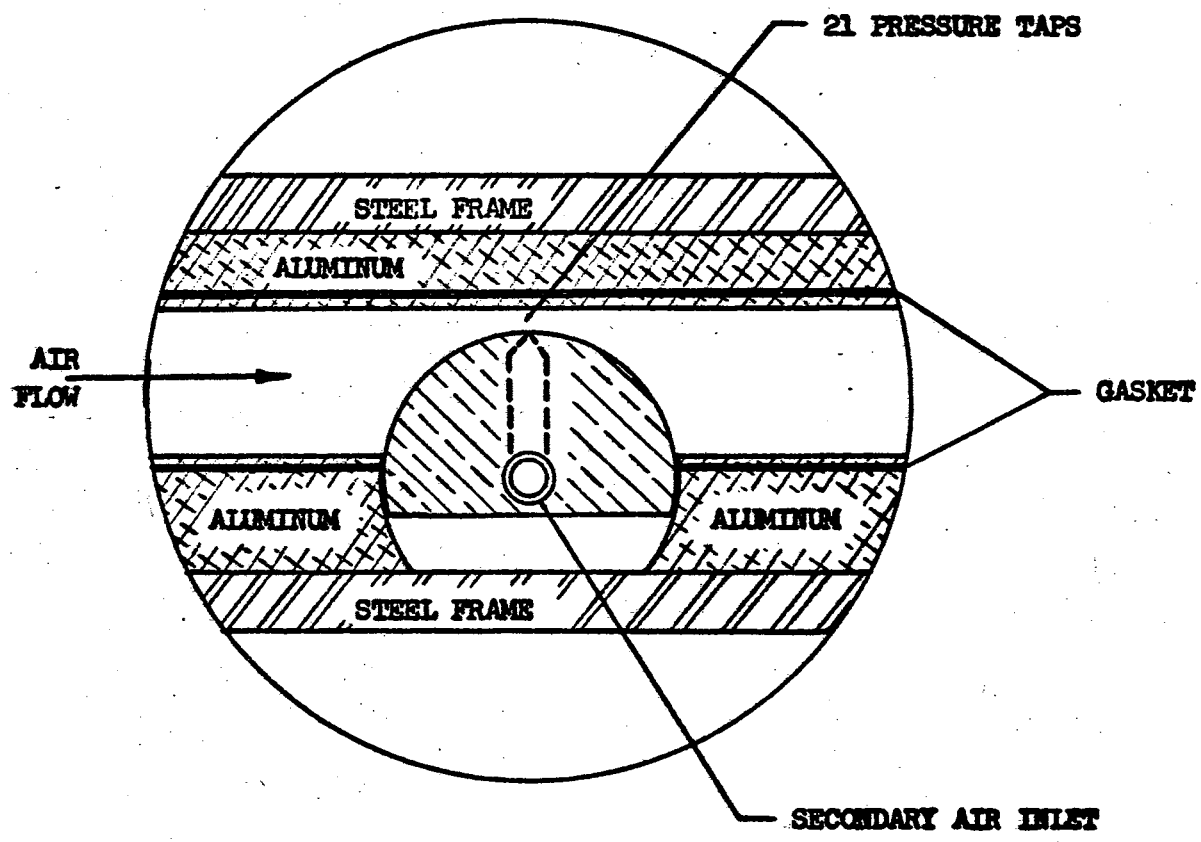

Figure 2-a. Detail of Test Section.

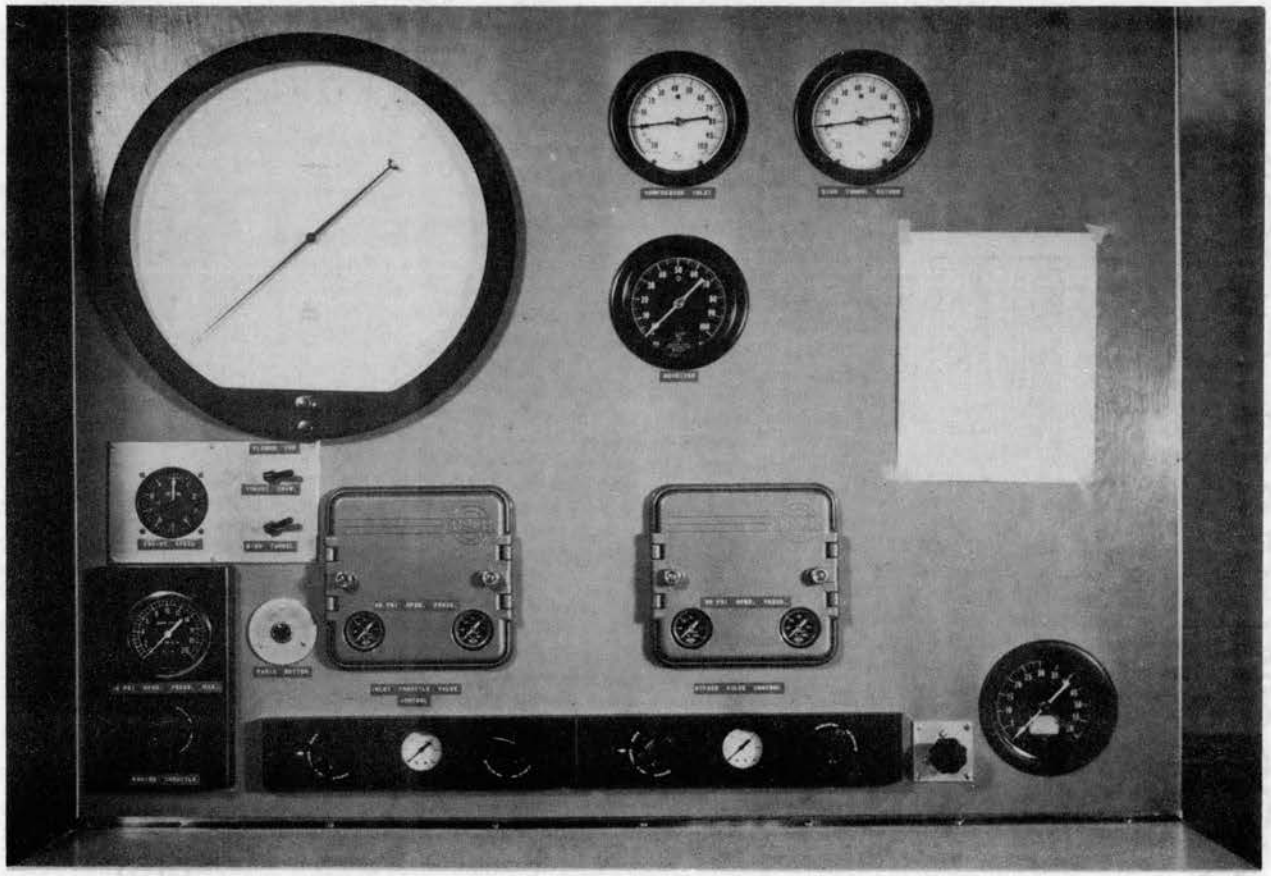

Figure 3. Control Panel for Test Equipment.

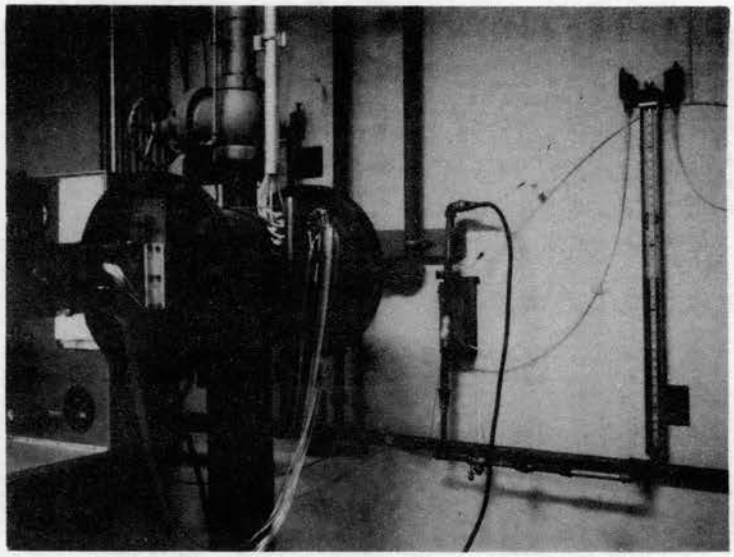

Figure 4. Test Equipment Showing Right Side and Two-position Valve.

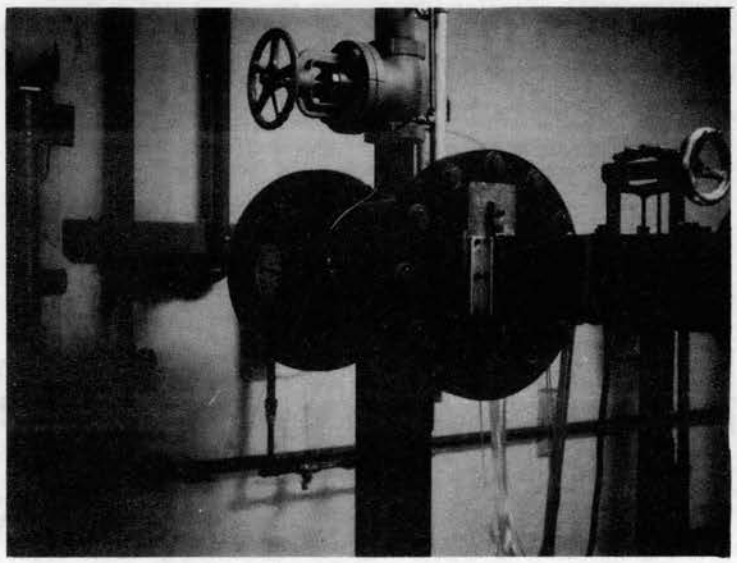

Figure 5. Test Equipment Showing Left Side and Settling Chamber.

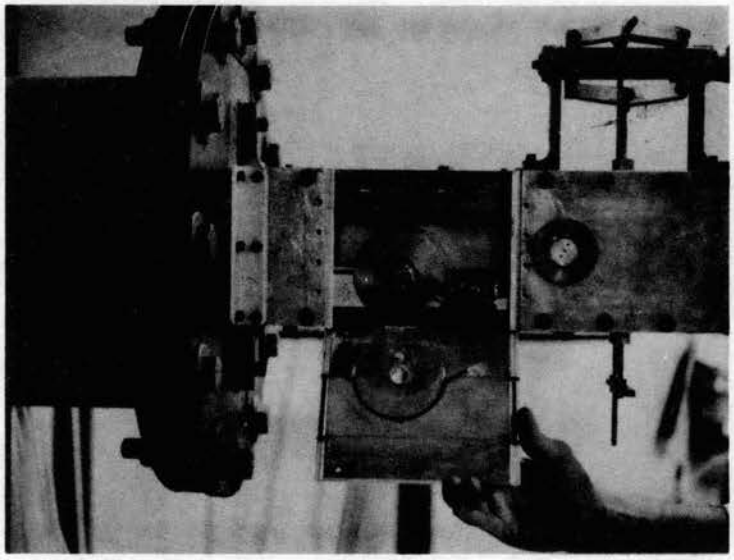

Figure 6. Throat Section, Nozzle Block and Left Side Wall.

The brass nozzle block had a 0.006 inch transverse slit for injection of the secondary fluid (Figure 2a). Secondary air was fed through the hollow 5/8 inch pivot shaft into the hollow chamber in the block and then through the converging slit into the main stream. Bearing surfaces for the nozzle block shaft were provided by the aluminum side walls.

Three rows of seven pressure taps each were located in the right side wall (as one faces upstream) in the throat area. The hole diameters were approximately 0.057 inches with a spacing of 0.150 inches horizontally and 0.125 inches vertically. The lower pressure tap in the first and last column were 0.150 inches below the center row and are shown in Figure 11, with the typical dimensionless pressures which will be discussed in Chapter V. Pressure taps were also drilled in the nozzle block fore and aft of the slit, 0.170 and 0.150 inches, respectively. These two taps were located 0.188 inches from the left side wall.

Since twenty pressure readings were required and only a ten-tube manometer bank was available, a special switching valve was designed and built. It consisted of a rotating disk with ten holes which was "sandwiched" between two flat plates. The rear plate had ten holes which were connected to the manometer tubes, and the front plate had twenty holes with hypodermic tubes to receive the pressure inputs. An exploded view of this valve is shown in Figure 7. In one rotary position, the center disk aligned ten of the pressure inputs to the manometer tubes, while in the other position the other ten inputs were connected to the manometer. At the intermediate rotary position, the manometer tubes were sealed off. This was, in effect, a series of ten

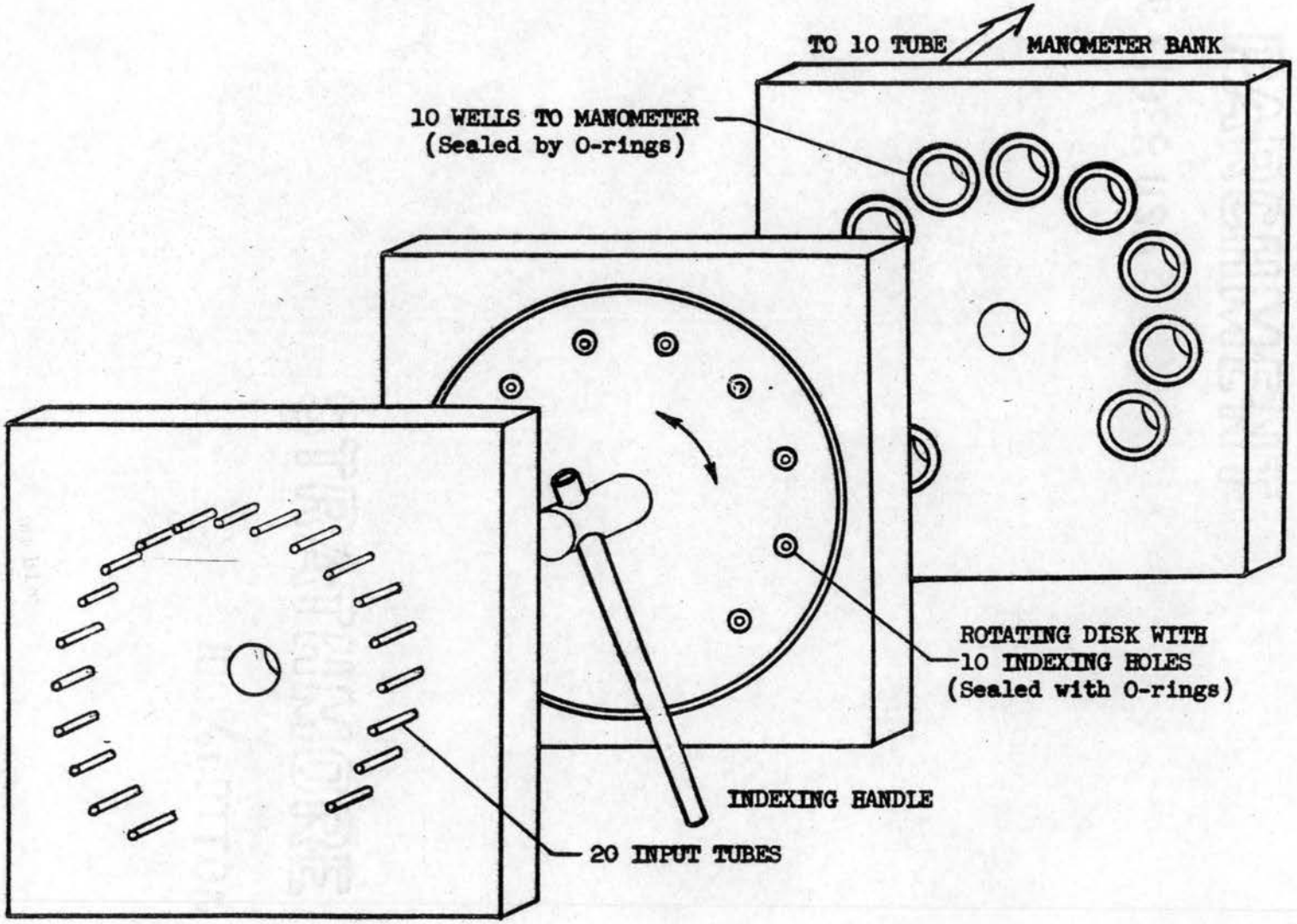

Figure 7. Exploded View of Switching Valve.

three-position valves. Pressure measurements from the first column of upstream taps were not made except for runs when the slit was rotated upstream of the throat more than 6 degrees, at which time the last column of downstream taps were not used.

Main flow measurements were made by the use of a 3.150 inch diameter sharp-edge orifice plate located in a 4 inch pipe downstream of an air reservoir, where the air was near settling chamber temperature and a pressure of about 50 psig. This orifice plate was calibrated against an ASME long radius metering nozzle which is in another section of the Gas Dynamics facility. Calibration curves were drawn with the mass flow as a function of the reservoir supply pressure and the pressure drop across the orifice plate. Secondary flow measurements were made with a 0.280 inch diameter sharp-edge orifice plate in the 3/4 inch stainless steel tubing. This orifice plate had been previously calibrated by Jackomis (6) in July 1962. Differential oil manometers were used to measure the pressure drop across each of these orifice plates.

A standard Heise gage was used to measure the stagnation pressure of each air supply. The stagnation temperature and pressure of the main flow were taken in the settling chamber just upstream of the test section. The temperature and pressure of the secondary air supply were taken in the 3/4 inch pipe near the metering orifice.

Sealing of the tunnel walls was a problem because of the three-piece construction of the lower section (Figure 2a) and the requirement for removable walls. It was necessary to have removable walls in order to rotate the nozzle block and to determine accurately the position of the slit. Sealing of the aluminum blocks was by O-ring material in channeled grooves. The brass nozzle block was sealed on the sides by

O-ring material in the side walls (Figure 6) and on the ends by the O-ring material in the aluminum blocks.

Through the use of O-ring material, leaks upstream and in the test section were eliminated. Leaks still prevailed downstream of the test section. Leaks in this area did not affect the test since mass flow rates were regulated by the effective throat area.

CHAPTER IV

TESTING PROCEDURE

The wind tunnel had continuous flow with a single return loop. Primary air flow was metered through the orifice plate from a reservoir at approximately 50 psig; it then passed through a throttling valve and into the settling chamber where the pressure was maintained at 26 psig. These pressures were used for ease in maintaining a constant airflow output and a positive gage pressure on each pressure tap and hence on the manometer bank. The air temperature was maintained near ambient through the use of two heat exchangers after compression.

The secondary air was supplied from a separate compressor and fed into the hollow nozzle block with a range of 0-140 psig. Control of this stagnation pressure was on a quasi-steady basis since the compressor governor was of the on-off type, and the pressure varied as much as 5 psi at the compressor. However, the discharge area for secondary injection was small, the compressor reservoir was large, and the pressure was reduced through valves and long pipes; hence, the pressure at the test section varied slowly. During the tests, after stabilization of the main flow, the secondary supply pressure was monitored and read first.

Since each system was controlled independently, it required about ten minutes for stabilization of the main flow once a fixed secondary pressure was selected. Air was bled from the primary reservoir to

compensate for the blockage by secondary injection as this proved easier than engine speed control for the small changes in the primary mass flow rate. Using part of the main supply air as the secondary injection fluid would probably make stabilization easier, however, this would limit the pressure available for the secondary flow.

The pressure of approximately 26 psig in the settling chamber gave about 25 inches of mercury deflection on the maximum test section static pressure pickup and about minus 6 inches (gage) on the minimum. This worked satisfactorily on the 50 inch mercury manometer board using an atmospheric reference pressure.

Lines from the pressure pickup in the side wall which led through the switching valve and into the manometer were checked for leaks. Using a positive pressure, the losses were less than 0.1 inch of mercury per minute. The manometer tubes were checked for equal pressure readings and checked within 0.1 inch. For the steady flow conditions of these tests, this was considered adequate.

The ratios of secondary-to-primary stagnation pressure used were: no flow, 0.6, 1, 1.5, 2, 2.5, 3, 3.5, and 4. When the slit was upstream of the throat, the minimum secondary stagnation pressure had to be greater than 0.6 in order to get some secondary flow.

Secondary mass flow rates were made dimensionless by establishing a ratio of $\dot{m}_2$ to $\dot{m}_o$, where $\dot{m}_o$ is the mass flow rate which would occur with no secondary injection at the same primary stagnation conditions. To achieve the variation in the mass flow ratio, the stagnation pressure ratio was varied.

The slit for injection was positioned at 4, 8 and 12 degrees upstream of the throat, at the throat, and 4 and 8 degrees downstream of the throat.

Determination of the slit location by an external pointer proved unsatisfactory, so it was necessary to remove the side wall to measure the slit location with a protractor. At the completion of the tests at each position, the slit position was again measured.

Pictures were taken of the manometer bank with a Polaroid Land camera for no secondary flow and for stagnation pressure ratios of 1, 2, and 3. These pictures were used for the determination of the static pressure field in the vicinity of the throat.

CHAPTER V

DISCUSSION OF RESULTS

When a secondary fluid is injected at or near the throat of a converging-diverging channel, the streamlines of the main flow diverge away from the convex wall and give an effective decrease in the throat area. This type of area control is called an aerodynamically-variable throat.

This study explored the most effective location for secondary injection normal to the convex wall. Previous studies on rocket nozzle area control by secondary injection were limited to injection at the physical throat. In order to study the flow pattern created with secondary injection and to determine the most effective injection position, a two-dimensional arc shape half-nozzle was used. This permitted secondary injection at any position without changing the shape of the nozzle.

Flow calculation through the rectangular nozzle, with no secondary injection and with the slit at the throat, resulted in a discharge coefficient of 0.971. The discharge coefficient increased to 0.976 when the slit was rotated upstream 4 degrees. The slit at the throat caused a disturbance to the flow which had the same effect as a step for reduction in the flow area, thereby lowering the C_d. At all other positions tested, the C_d was 0.989.

Figures 8 and 9 show the per cent change in primary mass flow versus the per cent of secondary injection. This is equivalent to the per cent change in primary flow area versus per cent of secondary injection. The magnification ratio is represented as the slope of the lines in these figures, since it was defined as the change in primary mass flow per unit secondary mass flow. Upstream injection is shown in Figure 8 and downstream injection in Figure 9, with throat injection shown in each figure for comparison.

The use of secondary injection is attractive since a blockage magnification ratio of about 2 to 1 was obtained when injection was at or near the physical throat. Similar results were obtained by Jackomis (6) when he used throat injection in an axisymmetric rocket nozzle. It is clearly evident that upstream injection is far more effective for throat area control than downstream injection. The reduction of throat area as a function of injection position, for three secondary-to-primary mass flow ratios, is shown in Figure 10. This was made by cross-plotting the data from Figures 8 and 9. The optimum injection position was the same in each case. Optimum injection for blockage effectiveness is near 4 degrees upstream of the physical throat. It appears that increasing the secondary-to-primary mass flow ratio does not alter this optimum injection position. However, this position may not be valid for different R/h ratios.

The magnification ratio varied from 1 1/2 to 1 at very low secondary mass flow rates to more than 2 to 1 as the secondary flow increased to 6 per cent of the primary flow when the injection was near the optimum position. The magnification ratio falls to unity when injection is more than 12 degrees upstream of the throat, although it may still be

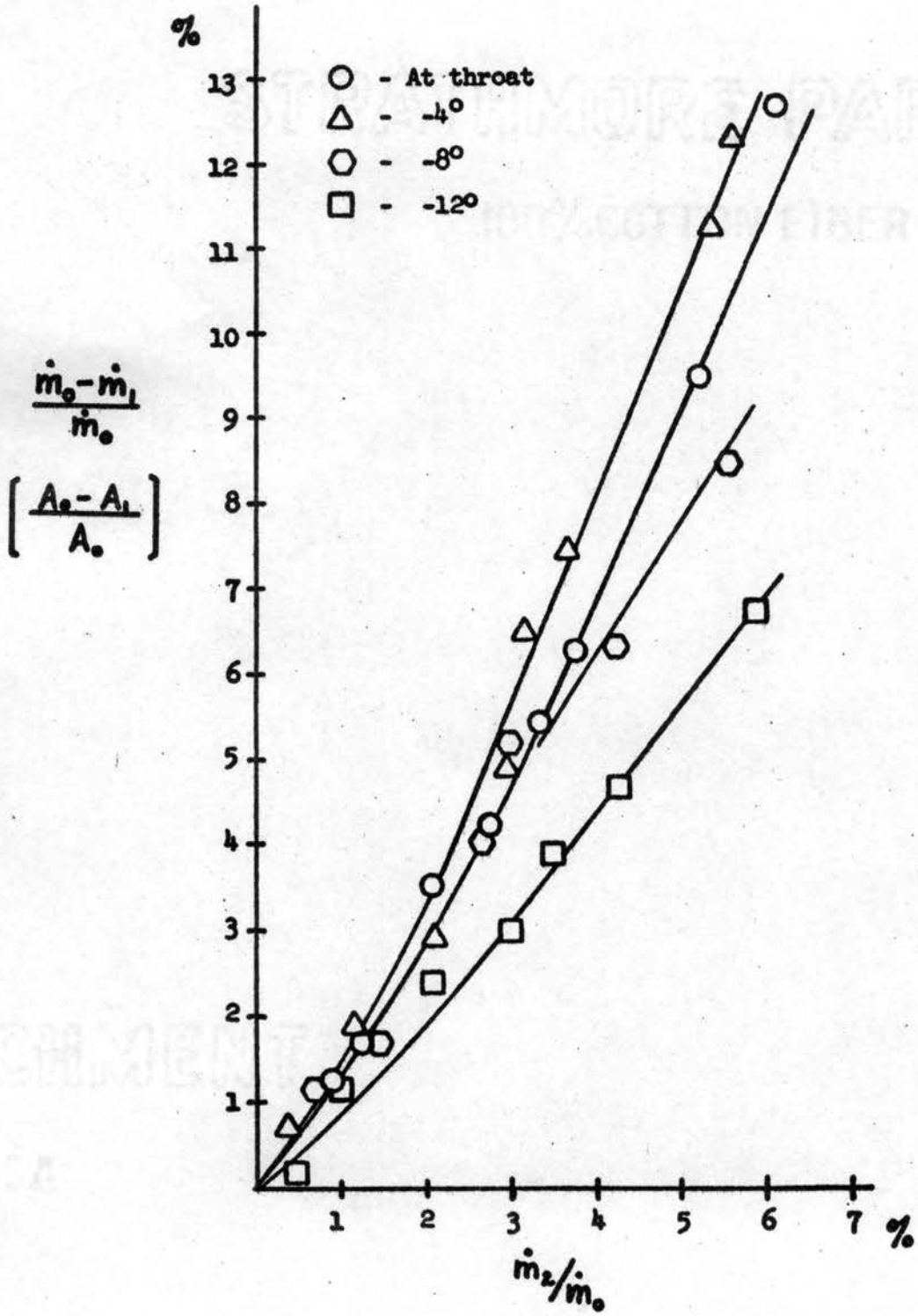

Figure 8. Reduction in Throat Area Versus Secondary Mass Flow (Upstream Injection).

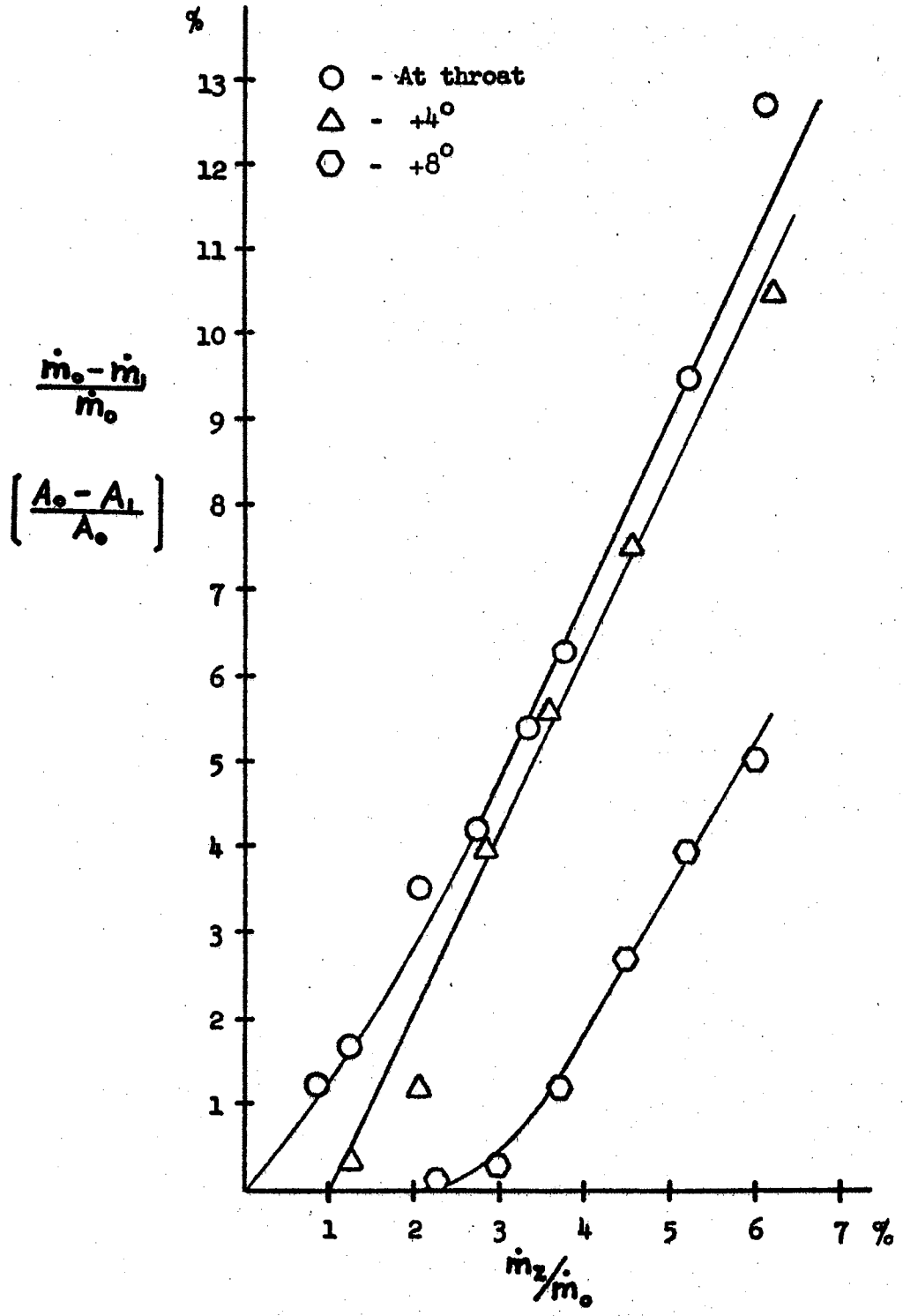

Figure 9. Reduction in Throat Area Versus Secondary Mass Flow (Downstream Injection).

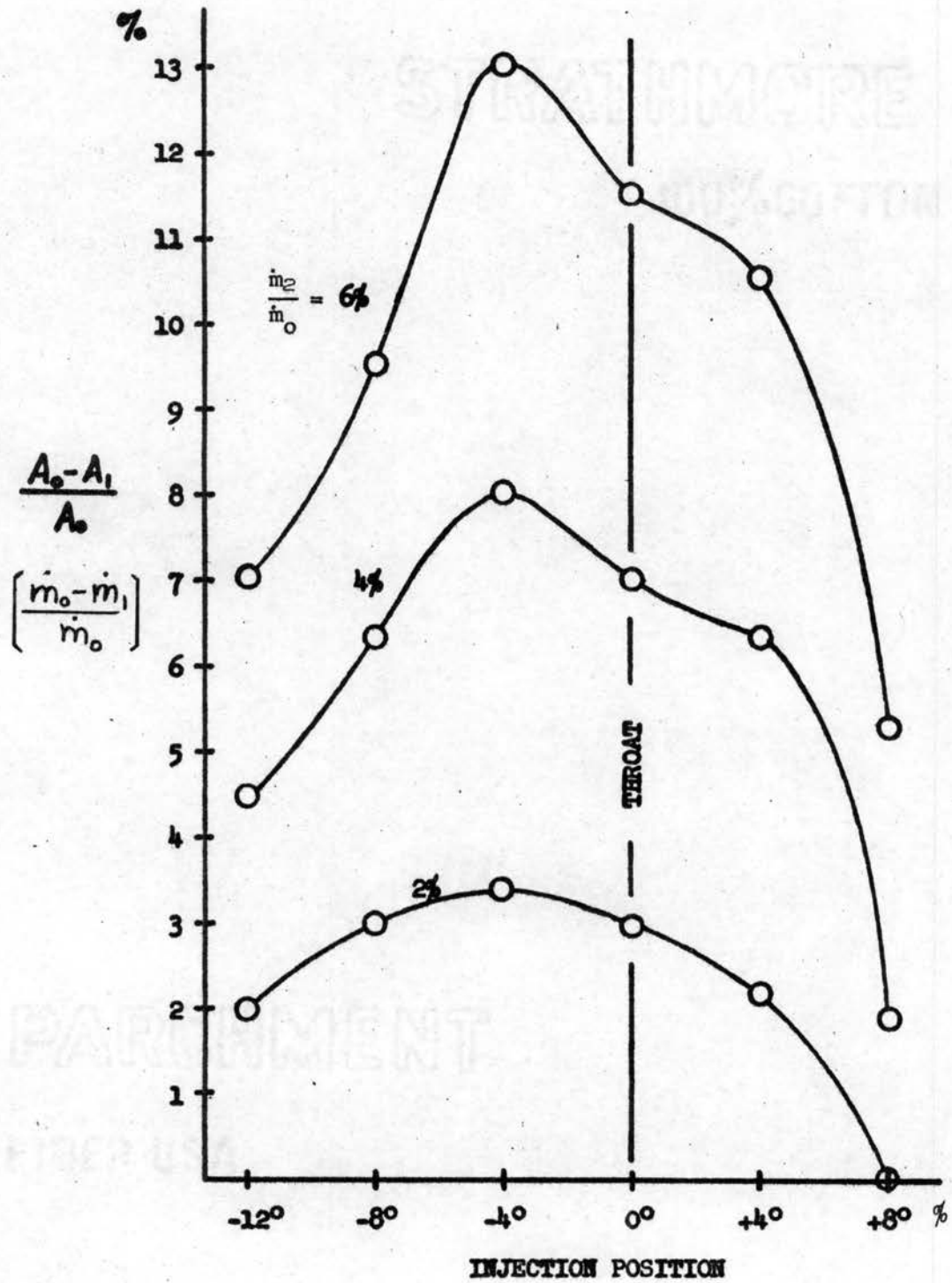

Figure 10. Reduction in Throat Area Versus Injection Position.

useful for boundary layer shielding of the nozzle throat.

Injection at the throat and injection 6 degrees upstream of the throat closely parallel each other in blockage effectiveness. However, when consideration is given to cooling of the nozzle throat, the 4 to 6 degree upstream position seems to offer the area of greatest usefulness.

The above conclusions regarding magnification ratio rest upon the experimental results. In examining the testing technique, some inaccuracies were involved and must be considered. Secondary stagnation pressure was assumed to be the same as the static pressure in the 3/4 inch pipe line since the velocity was less than 15 feet per second. However, downstream of the pressure measurement, a long 1/4 inch pressure hose was used to supply the secondary air to the nozzle block. Fanno line calculations indicate that hose pressure losses caused about an 8 per cent decrease in the stagnation pressure supplied to the nozzle block. This was realized after the completion of the tests and therefore the stagnation pressure ratios shown in Figure 11 are approximately 8 per cent high. This does not change the magnification ratios since the pressure loss does not affect the mass flow calculations.

The accuracy of the primary mass flow rate measurement was poor since the air reservoir remote pressure gage had a slow response time and 2 psi graduations. One graduation corresponded to a change of 1.5 per cent of the mass flow as read from the calibration curve, discussed in Chapter III. A more accurate gage for measurement of the pressure at the main sharp-edge orifice would improve the accuracy of the primary flow measurements and hence the accuracy of the magnification ratios. Secondary mass flow measurements used the Heise gage for total pressure which had 1/2 psi graduations and a much faster response.

The determination of the injection position was not a problem as it was easily set and measured to within 30 minutes of arc. External determination of the injection position proved unsatisfactory.

Plotting the dimensionless pressure field (Table I and Figure 11) permits the calculation of the velocity, and Mach number at various points in the flow field when there is no secondary injection. As the secondary flow is introduced, the determination of the lines of constant velocity is not possible unless the interface between the two fluids is known. It was hoped that the overpressure of the injected fluid would permit the determination of the blockage pattern and thereby lead to the shape of the main stream flow.

After stabilization of the two flows, the presence of the secondary gas did not cause any significant change in the pressure field. Examination of the results indicate that blockage was due to the momentum deficiency of the secondary fluid in the axial direction rather than to major alteration of the pressure field. Therefore, it is probable that the region of low pressure and separation, immediately downstream of the slit, occurs within a few slit widths. The closest pressure pickup in the axial direction was downstream 25 slit widths and did not reflect a pressure change. Measurement of this phenomena was hindered by the fact that the diameter of the taps was about ten slit widths, and that the taps average the pressure field over their area.

Initial axial momentum of the secondary fluid may change the blockage effectiveness, but to date, injection has been near the throat and the injection angles relatively small. For this reason, no correlation to slit width has been noted. The use of an injection position more than ten degrees upstream of the throat should be accompanied by a

Stagnation Pressure Ratio	Row \ Column	1	2	3	4	5	6	7
1.00	I	x	.746	.6875	.619	.459	.426	.360
	II	x	.736	.6785	.610	.469	.405	.456
	III	x	.713	.659	.614	.440	.369	*
1.50	I	x	.764	.707	.649	.503	.416	.358
	II	x	.754	.697	.623	.447	.399	.333
	III	x	.742	.688	.627	.421	.366	.294
1.97	I	x	.770	.716	.645	.503	.396	.346
	II	x	.760	.715	.638	.434	.404	.322
	III	x	.741	.709	.639	.380	.370	.288

x taps not used

* reading missed

Dimensionless pressures are expressed as P/P_{o1}.

Table I. Dimensionless Static Pressure Field with Injection at the Throat.

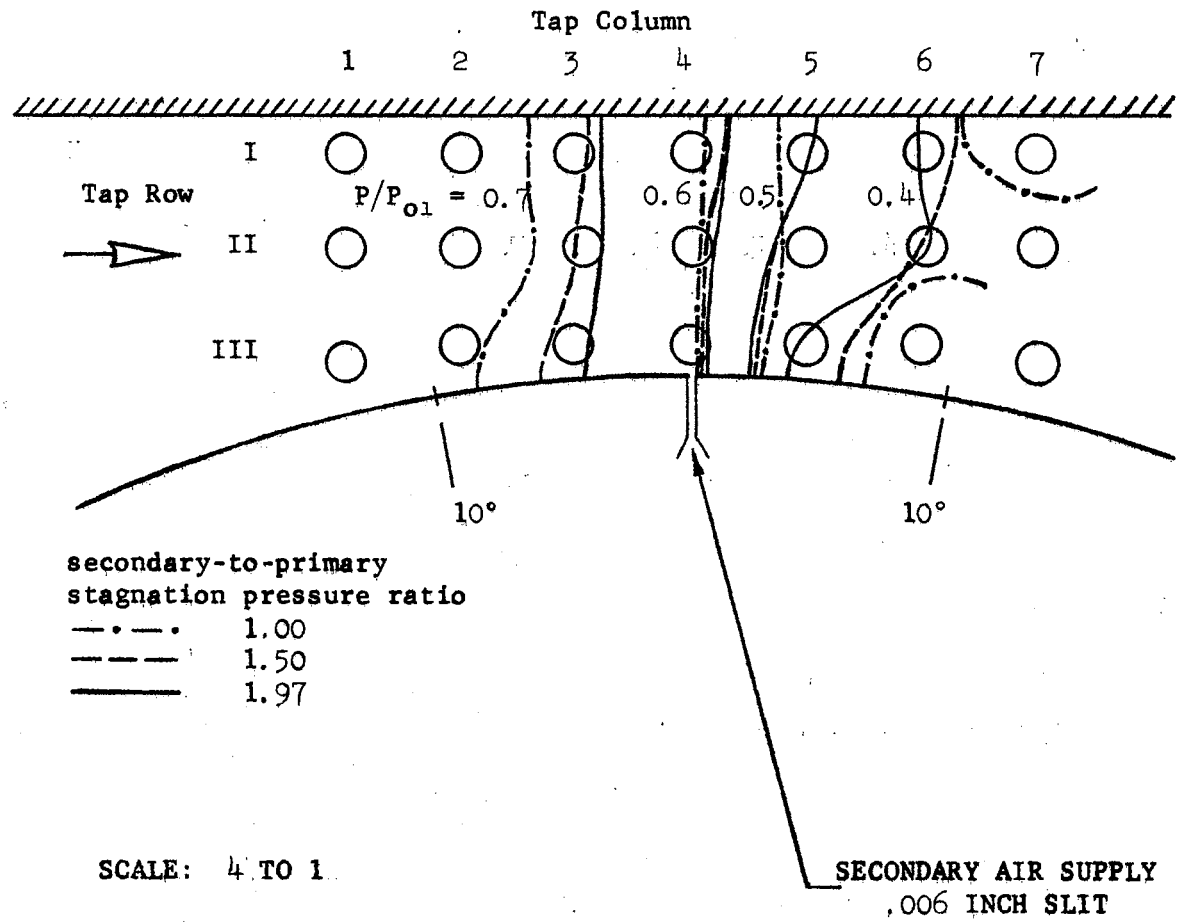

Figure 11. Dimensionless Static Pressure Field with Injection at the Throat.

measurable thrust loss, and the increased mixing of the gases would tend to reduce the thermal protection of the secondary gas. Investigation of the axial momentum effects on blockage should be made using the 4 degree upstream of the throat position, with varying injection angles and slit widths.

In applying these results to rocket nozzles, it must be remembered that generally different gases will be used. This will also mean different stagnation pressures and temperatures. With the different gases the density of the secondary fluid is almost certain to be greater, since it would be the cooler, and since low molecular weight exhaust gas in the primary stream gives higher specific impulse. This would permit greater secondary-to-primary mass flow rates using the same slit width. But, if one can conclude that the principle parameter is the mass flow ratio of the two streams, then the results should be similar.

Further studies of the flow field using Schlieren photography and water table analogy are planned. When more is known about the interface and the extent of mixing, data taken on the pressure field during this study should prove useful.

CHAPTER VI

CONCLUSIONS

The optimum position for secondary injection in a two-dimensional converging-diverging nozzle with an arc shape throat is four degrees upstream of the throat. This results in a magnification ratio of more than two to one. However, this may be a function of the throat height versus the radius of curvature of the nozzle (5.6 to 1 in this study).

The optimum position for injection was unaffected by the amount of secondary mass flow for secondary-to-primary mass flow ratios from zero to six per cent.

The sensitivity for positioning of the slit for maximum magnification is greater at higher secondary mass flow rates.

The pressure field changes caused by secondary injection occur locally in the slit area, and the pressures are equalized across the interface of the two fluids a short distance downstream of the injection point.

RECOMMENDATIONS

A different secondary fluid should be injected and Schlieren pictures taken to determine the interface position and the extent of mixing. Water table analogy of secondary injection should also prove useful, where it would be possible to use similar or different injection fluids. Coloring the secondary fluid would help show the extent of mixing and

the turbulence along the interface.

The pressure field near the injection slit should be examined more closely, since a separated flow region exists fore and aft of the slit as shown by the water table analogy (7). Smaller diameter pressure pickups should be used as the diameter of the ports were 17 per cent of the throat height.

Tests should be performed having the secondary injection directed upstream at considerable angles. If the optimum injection position, four degrees upstream with this test equipment, were used then the effect of initial axial momentum of the secondary fluid would show up as changes in the magnification ratio.

SELECTED BIBLIOGRAPHY

1. Berman, K. and F. W. Crimp, Jr., "Performance of Plug-Type Rocket Exhaust Nozzles," A.R.S. Journal, January 1961.

2. Gates, J. S. and S. L. Pinto, "Thrust Magnitude Control for Solid Propellant Rocket Motors by Mechanical Means," S.A.E. Paper T-59.

3. Rao, G. V. R., "The E-D Nozzle," Astronautics, September 1960.

4. Zumwalt, G. W. and W. N. Jackomis, "A Secondary Injection Nozzle for Solid Rocket Thrust Magnitude Control," A.R.S. Solid Propellant Rocket Conference, April, 1962, Paper 2337-62.

5. Zumwalt, G. W. and W. N. Jackomis, "Aerodynamic Throat Nozzle for Thrust Magnitude Control of Solid Fuel Rockets," A.R.S. Journal December 1962, pp. 1934-1936.

6. Jackomis, W. N., "An Experimental Study of Aerodynamically Variable Throat Area (AVT) Nozzles," M. S. Thesis, Oklahoma State University, August 1962.

7. Stutzman, R. D., "Investigation of Secondary Injection Using the Hydraulic Analogy." Unpublished Report, School of Mechanical Engineering, Oklahoma State University, May, 1963.

8. Rodriguez, C. J., "An Experimental Investigation of Jet-Induced Thrust Vector Control Methods." Proc. of the 17th Annual JANAF Solid Propellant Meeting, Denver, Colo., May, 1961.

9. Martin, A. I., "The Aerodynamically Variable Nozzle," Journal of Aerospace Science, May 1957, pp. 357-362.

10. Bankston, L.T. and G. G. Barnes, "Thrust Vectoring: Shock and Pressure Effects of Cold Air Injection into a Two-Dimensional Nozzle," NOTS Tech. Publication 2608, Naval Ordnance Test Station, China Lake, California, January 1961.

APPENDIX A

The boundary layer thickness on the solid centerline and on the side walls, with no pressure gradient, would be:[1]

$$\delta \sqrt[5]{Re_x} = 0.37\ x$$

where x = distance from leading edge

Re_x = local Reynolds number

with the displacement thickness defined as:[2]

$$U\delta^* = \int_0^\infty (U-u)dy$$

where u = local velocity

U = free stream velocity.

The relationship of displacement thickness to boundary layer thickness for turbulent boundary layers is given by:[3]

$$\delta \cong 6\delta^* .$$

The above equations predict a displacement thickness of 0.0233 inches at the throat of the test section or five per cent of the throat height. However, this assumes no pressure gradient; therefore, with the rapidly falling pressure field, the displacement thickness should

---

[1] Schlichting, H., Boundary Layer Theory, McGraw-Hill, New York, 1960, pp. 38.

[2] Ibid, pp. 27.

[3] Pope, A., Wind Tunnel Testing, John Wiley & Sons, New York, 1954, pp. 279.

be about one order of magnitude smaller or about one-half per cent.

Calculation of flow area reduction by flow coefficients resulted in a decrease of 1.1 per cent. This corresponds to a displacement thickness of 0.0014 inches at the throat. Thus, the assumption of a negligible boundary layer at the throat of the nozzle appears to be justified.

VITA

Roger O. Warloe

Candidate for the Degree of

Master of Science

Thesis: A STUDY OF SECONDARY AIR INJECTION INTO A TWO-DIMENSIONAL CONVERGING-DIVERGING NOZZLE

Major Field: Mechanical Engineering (Aeronautical)

Biographical:

Personal Data: Born in Los Angeles, California, April 17, 1932, the son of Harold P. and Elsie E. Warloe.

Education: Attended grade school in Los Angeles, California; graduated from Manual Arts High School, Los Angeles, California in 1950; received the Bachelor of Arts degree from the University of California at Los Angeles, with a major in physics, in January 1955; completed requirements for the Master of Science degree at Oklahoma State University in August, 1963.

Professional experience: summer work as engineering assistant, 1954, Naval Ordnance Test Station, China Lake, California; Physicist at NOTS in 1955 for 3 months; came on active duty with U. S. Air Force in May, 1955 and graduated from flying school as a pilot in June, 1956.